Laser-Driven Micro Transfer Placement of Prefabricated Microstructures

Reza Saeidpourazar, Rui Li, Yuhang Li, Michael D. Sangid, *Member, ASME*, Chaofeng Lü, Yonggang Huang, John A. Rogers, *Fellow, IEEE*, and Placid M. Ferreira

***Abstract*—Microassembly of prefabricated structures and devices is emerging as key process technology for realizing heterogeneous integration and high-performance flexible and stretchable electronics. Here, we report on a laser-driven micro transfer placement process that exploits, instead of ablation, the mismatch in thermomechanical response at the interface of a transferable microstructure and a transfer tool to a laser pulse to drive the release of the microstructure from the transfer tool and its travel to a receiving substrate. The resulting facile pick-and-place process is demonstrated with the assembling of 3-D microstructures and the placement of GaN light-emitting diodes onto silicon and glass substrates. High-speed photography is used to provide experimental evidence of thermomechanically driven release. Experiments are used to measure the laser flux incident on the interface. These, when used in numerical and analytical models, suggest that temperatures reached during the process are enough to produce strain energy release rates to drive delamination of the microstructure from the transfer tool. [2011-0274]**

***Index Terms*—Chip-scale packaging, flexible electronics, microassembly, micro-manipulation, printed microelectromechanical systems.**

Manuscript received September 24, 2011; revised March 19, 2012; accepted March 27, 2012. Date of publication July 5, 2012; date of current version September 27, 2012. Subject Editor C. Hierold.

R. Saeidpourazar is with Brooks Automation, Inc., Chelmsford, MA 01824 USA (email: saeidpour@gmail.com).

R. Li is with the Faculty of Infrastructure Engineering, Dalian University of Technology, Dalian 116024, China, and also with the Department of Civil and Environmental Engineering and the Department of Mechanical Engineering, Northwestern University, Evanston, IL 60208 USA (e-mail: ruili19851985@yahoo.com).

Y. Li is with the Department of Civil and Environmental Engineering and the Department of Mechanical Engineering, Northwestern University, Evanston, IL 60208 USA, and also with the School of Astronautics, Harbin Institute of Technology, Harbin 150001, China.

M. D. Sangid is with the School of Aeronautics and Astronautics, Purdue University, West Lafayette, IN 47907-2045 USA (email: msangid@purdue.edu).

C. Lü was with the Department of Civil and Environmental Engineering and the Department of Mechanical Engineering, Northwestern University, Evanston, IL 60208 USA. He is now with the Soft Matter Research Center and the Department of Civil Engineering, Zhejiang University, Hangzhou 310058, China.

Y. Huang is with the Department of Civil and Environmental Engineering and the Department of Mechanical Engineering, Northwestern University, Evanston, IL 60208 USA (e-mail: y-huang@northwestern.edu).

J. A. Rogers is with the Department of Materials Science and Engineering, the Beckman Institute for Advanced Science and Technology, and the Frederick Seitz Materials Research Laboratory, University of Illinois at Urbana–Champaign, Urbana, IL 61801 USA (e-mail: jrogers@illinois.edu).

P. M. Ferreira is with the Department of Mechanical Science and Engineering, University of Illinois at Urbana–Champaign, Urbana, IL 61801 USA (e-mail: pferreir@illinois.edu).

Color versions of one or more of the figures in this paper are available online at http://ieeexplore.ieee.org.

Digital Object Identifier 10.1109/JMEMS.2012.2203097

I. Introduction

THIS PAPER develops and characterizes a facile laser-driven transfer assembly process that transfers prefabricated micro- and nanostructures/devices from the growth/fabrication substrates to functional substrates incapable of supporting their growth and/or fabrication processes. In terms of emerging technologies, the process described in this paper extends the capabilities of mechanical transfer printing [1]–[5], a process that has already demonstrated a new manufacturing pathway to embedding high-performance electronic and optoelectronic components into polymeric substrates to realize new capabilities in emerging areas such as flexible and large-area electronics, displays, and photovoltaics.

Fig. 1 shows examples of systems such as epidermal electronic patches [1], flexible photovoltaic microcells [2], hemispherical focal arrays for an electronic eye [3], stretchable light-emitting diode (LED)-based lighting [4], and backplanes for active matrix organic LED (OLED) displays [5] in which transfer printing was the primary enabling process. Such devices would be difficult, if not impossible, to realize by conventional approaches. The reader is referred to [1]–[5], [9]–[13], and [15] for more information on transfer printing, a process in which conventional lithography-based fabrication techniques are used to fabricate dense arrays of functional microstructures (thin-film transistors, microscale LEDs, etc.) that are partially released by undercut etching from their growth or handle substrate. This becomes the donor substrate or "inking pad." An elastomeric transfer tool or "stamp" is micropatterned so as to selectively make contact with individual microstructures on the donor substrate and, exploiting the adhesion with its compliant surface, extract them from the donor. These microstructures are then deposited on the functional or receiving substrate by bringing them into contact. Release of the microstructures from the stamp is achieved by kinetic modulation of the adhesion energy at the interface or with the use of adhesives on the receiving substrate. Within this context of transfer printing, laser-driven transfer placement provides a noncontact mode of transferring the microstructures from the transfer tool or stamp to the receiving substrate. As a result, the success of the transfer process is relatively independent of the topography, properties, and preparation of the surface of the receiving surface.

With respect to more conventional processes, the process described here has the potential to add to the capabilities of bare-die assembly processes. It adds sub-50-μm die-placement capabilities and provides for the possibility of noncontact placement with soft tooling. It also allows for the placement of

1057-7157/$31.00 © 2012 IEEE

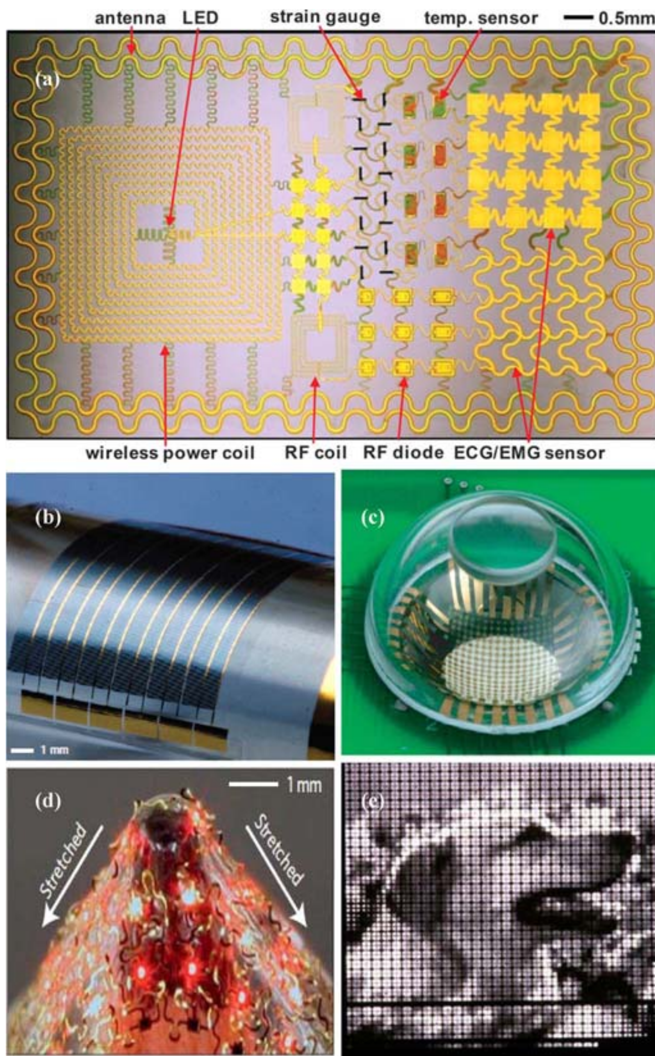

Fig. 1. Examples of devices made using transfer printing. (a) Epidermal patch for biomonitoring [1]. (b) Flexible ultrathin silicon solar microcells [2]. (c) Electronic eye camera [3]. (d) LEDs on a stretchable polymeric substrate [4]. (e) OLED display with transfer printed backplane [5].

microstructures and devices without attached handle substrate material. For this paper, we shall refer to the microstructures being transferred during this process as "chiplets" to indicate that, in general, we expect them to be smaller and thinner than a chip. The physical object that is used to pick up and deposit the chiplets will be referred to as the transfer tool. Finally, the growth/fabrication substrate from which the chiplets are extracted is called the donor substrate, and the functional substrate onto which it is deposited is called the receiving substrate.

Viewed from the perspective of laser-based processing technology (Wartena *et al.* [6] capture a portion of the vast diversity of laser-based processing in a succinct categorization of laser direct write (LDW) processing), the process that we develop in this paper belongs to the category of LDW addition and, more specifically, to what is referred to as laser-induced forward transfer (LIFT) or laser-driven release. This type of transfer process was first reported by Bohandy *et al.* [7]. LIFT-type processes have also been used to assemble or place prefabricated microstructures. Holmes and Saidam [8], calling the approach laser-driven release, used it for batch assembly in microelectromechanical systems (MEMS) fabrication.

Unlike all other variants of the LIFT process associated with transferring prefabricated microstructures, the process suggested here does not use laser ablation of a sacrificial layer at the interface of the transfer tool and the chiplet to drive the transfer. Instead, it exploits a mismatched thermomechanical response of the chiplet and the transfer tool to a laser pulse incident on the transfer-tool–chiplet interface to cause the delamination of the chiplet from the transfer tool and its transfer to the receiving substrate. This allows for a process that operates at lower temperatures, thus avoiding any damage to the functional chiplets. More importantly, because the transfer does not damage the transfer tool, it can be used multiple times, enabling a pick–place–repeat cycle. Like all the other LIFT processes described previously, this process uses a transfer tool that is transparent to the laser radiation being used. However, unlike the other LIFT processes, the transfer tool is made of soft patterned viscoelastic material [in this paper, polydimethylsiloxane (PDMS)]. Aside from providing the desired mismatch in thermomechanical response with commonly used semiconductor materials, patterned transfer tools of such materials also make it possible to directly and selectively pick up chiplets from donor substrates by using well-developed techniques from the Rogers laboratory [9]–[13]. This overcomes one of the major limitations of using LIFT-type printing processes for assembling microstructures, i.e., the transfer of the microstructures from the growth/fabrication substrate to the transfer tool or LIFT support substrate [14]. This process therefore combines the facile elegance of the transfer printing processes in transferring microstructures directly from their growth/fabrication substrates into functional substrates with the flexibility of the noncontact LIFT processes that are relatively independent of the surface properties and preparation of the functional substrate onto which they are transferred.

II. LMTP

A good starting reference for the development of this process is the transfer printing process as described by Mietl *et al.* [15] which involves both the pickup of chiplets from a donor substrate and their printing onto a receiving substrate using an elastomeric transfer tool. The process proposed here also starts with an elastomeric transfer tool made of the same material (PDMS) and patterned with posts, to selectively engage with the desired pattern of chiplets on the donor substrate. The mechanism for pickup of chiplets is essentially the same as that in [9]–[13], relying on the strong van der Waal forces between PDMS and the chiplet to extract it from the donor substrate. Additionally, the release of the chiplet from the handle layer of the donor substrate by undercut etching during fabrication aids the extraction of the chiplet from the donor substrate. For placement, however, the transfer tool is brought close (between 3 and 10 μm) to the receiving substrate onto which the chiplet is to be placed. A pulsed laser beam is focused on the interface of the transfer tool and the chiplet to release and drive it to the receiving substrate. The wavelength of the laser is chosen so that the transfer tool material is transparent, while the chiplet is

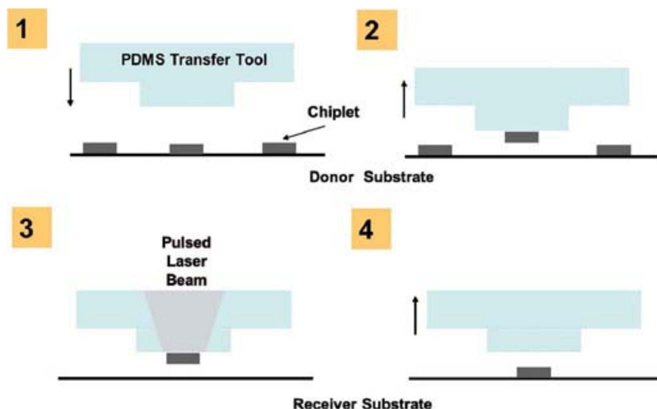

Fig. 2. Schematic of the laser transfer placement steps. (1) PDMS transfer tool is aligned with the donor substrate to pick up chiplets. (2) Chiplet is transferred to tool. (3) Transfer tool is aligned to a receiving substrate, and a laser pulse is used to heat up the chiplet–tool interface. (4) Chiplet is transferred to the receiving substrate.

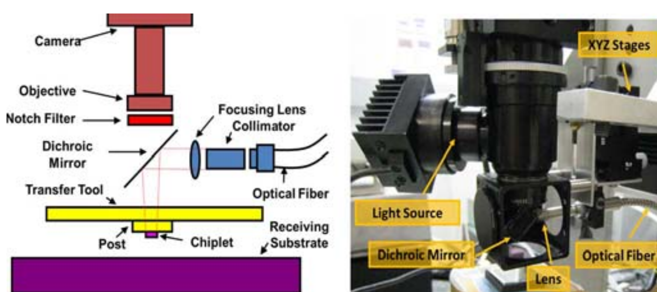

Fig. 3. Schematic depiction and photograph of the LMTP placement head. The laser beam is brought into the head by an optical fiber, bent and focused on the chiplet–tool interface. A dichroic mirror allows for the monitoring of the process with a high-speed camera positioned above the transfer tool.

more absorbing it. Fig. 2 shows a schematic of this noncontact laser-driven micro transfer placement (LMTP) process.

To realize this process, an LMTP placement head is assembled around an electronically pulsed 30-W 805-nm laser diode with a minimum pulsewidth of 1 ms. The laser is coupled into the system through a 250-μm core optical fiber. At the end of the fiber are a 4-mm-diameter collimator and a focusing lens with a 30-mm focal distance to focus the laser beam on a circular area with a diameter of approximately 400–800 μm. Fig. 3 shows a schematic and a photograph of the LMTP placement head. The laser beam is brought in through the side of the placement head, bent 90° by a dichroic mirror and focused onto the surface of a post (typically, 200 μm $\times$ 200 μm and 100 μm tall) patterned on the PDMS transfer tool. An objective directly above the transfer tool along with a charge-coupled device camera and suitable optics allows observation of the process with a pixel resolution of 1 μm.

The laser placement head is tested by using a 2 mm $\times$ 2 mm 1-mm-thick PDMS transfer tool with a 200 μm $\times$ 200 μm 100-μm-tall post patterned on it. The transfer tool is mounted onto a glass backing. For the chiplets, a donor substrate is fabricated using conventional fabrication processes [15] to obtain anchored, but undercut, 100 μm $\times$ 100 μm $\times$ 3 μm single-crystal silicon (SCS) squares. An automated placement machine is constructed by integrating a programmable computer-controlled xyz positioning stage, with the placement head, high-resolution optics, and vacuum chucks for the donor and receiving substrates. As shown in the process schematic in Fig. 2, the stage moves and locates the transfer tool to enable the pickup of a single chiplet. The stage is then moved to locate the chiplet directly above a receiving (for example, in Fig. 4(a), an RC1 cleaned patterned silicon substrate with 50-μm gold traces) substrate at a distance of 10 μm from it. The laser pulse time was set to 2 ms, and the laser power was gradually increased until delamination was observed. Fig. 4(a) shows the results of this placement experiment.

A second feasibility test is conducted to demonstrate the construction of 3-D assemblies using the LMTP process. Here, a three-layer pyramid of the same 100 μm $\times$ 100 μm $\times$ 3 μm silicon squares, shown in Fig. 4(b), is constructed. In a third test, simulating the placement of microstructures into other functional structures, the same square silicon chip is placed onto an atomic force microscope cantilever, something that would be difficult to achieve with other processes. Finally, Fig. 4(d) shows a 320-nm-thick silicon chip placed onto the structured surface. This verifies the claim that the process is independent of the properties of the receiving substrate and demonstrates the ability of the process to place ultrathin microstructures.

Transfer placement of an InGaN-based μ-LED onto a chemical vapor deposition (CVD)-grown polycrystalline diamond on a silicon substrate is shown in Fig. 5. These InGaN-based μ-LEDs consist of epitaxial layers on a (111) silicon wafer. The active device layers consist of p-type GaN layer (110 nm of GaN:Mg), multiple quantum well (5$\times$ InGaN/GaN:Si of 3 nm/ 10 nm), and n-type layer (1700 nm of GaN:Si). Metal layers of Ti/Al/Mo/Au (15 nm/60 nm/20 nm/100 nm) and Ni/Au (10 nm/10 nm) are deposited and annealed in optimized conditions to form ohmic contacts to n-GaN and p-GaN, respectively. These LEDs are placed on the receiving substrate by using a single 1-ms laser pulse. Fig. 5(a) shows an InGaN-based μ-LED placed on a structured silicon substrate, while Fig. 5(b) shows a schematic of the stacks of the InGaN-based μ-LED. Fig. 5(c) shows that μ-LED is functional after having been placed on a silicon substrate coated with a CVD-grown polycrystalline diamond film.

III. LMTP Mechanism and Experimental Observations

We have previously claimed that the primary phenomenon driving the LMTP process is not ablation but, instead, the mismatched thermomechanical responses of the transfer tool and the chiplet which causes the delamination of the chiplet from the transfer tool and its transfer to the receiving substrate. In this section, we describe the mechanism by which the chiplet is delaminated from the transfer tool and transferred to the receiving substrate and provide high-speed photography evidence in support of this mechanism.

Since a PDMS transfer tool is transparent in the near-infrared (IR) range, the laser radiation is transmitted through it and is incident on the chiplet which absorbs some fraction of the incident laser energy and, as a result, heats up. The chiplet,

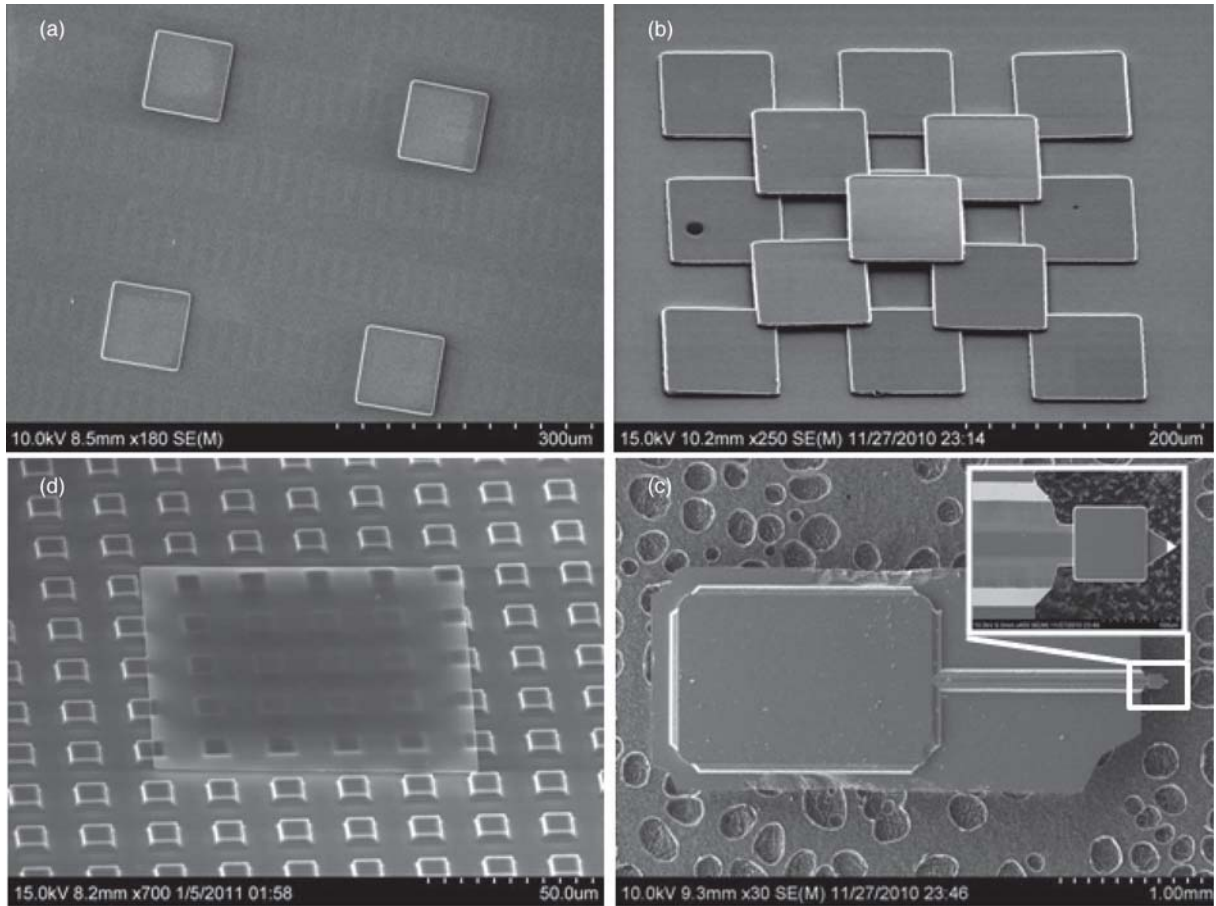

Fig. 4. Micrographs of examples of placement using the LMTP process. (a) 100 μm × 100 μm × 3 μm silicon squares placed between metallic traces on a silicon wafer. (b) Three-dimensional pyramid built with the same silicon squares. (c) Silicon square placed on a silicon cantilever. (d) 100 μm × 100 μm × 0.32 μm ultrathin Si square placed onto a structured substrate.

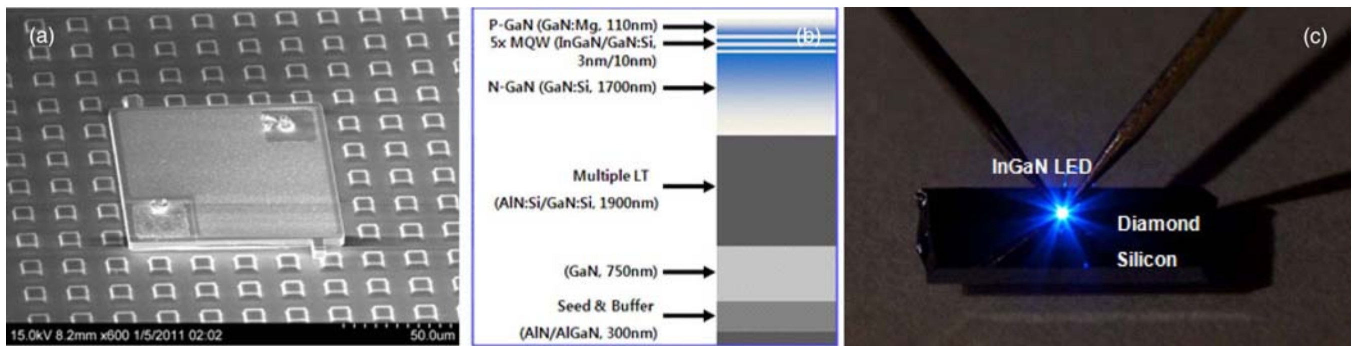

Fig. 5. Placement of InGaN-based μ-LEDs. (a) InGaN-based μ-LED placed onto a structured silicon substrate. (b) Schematic stacks of the InGaN-based μ-LED. (c) Functioning μ-LED placed on a CVD-grown polycrystalline diamond on silicon substrate.

in turn, acts as a heat source for the PDMS transfer tool, conducting heat across the tool–chiplet interface to raise the temperature of the PDMS in the vicinity of the interface. The rise of temperature in the PDMS and chiplet leads to thermal expansions in both. This, due to the considerable difference in the coefficients of thermal expansion for the two materials (310 ppm/°C [16] for PDMS and 2.6 ppm/°C for silicon [17]) and the restriction placed on their free expansion by the contact interface between them, must be accommodated by bending (or the formation of a curvature) in the PDMS–silicon composite. This stresses the interface, and when the energy release rate due to delamination at the interface exceeds the work of adhesion of the interface, the chiplet is released from the transfer tool. The increase in bending strain (and, hence, bending strain energy difference between the transfer tool and the chiplet) from the center of the chiplet to its boundaries and the stress concentration at the discontinuity caused by its boundary suggest that the delamination by this proposed mechanism will start at the outside boundary/corner of the chiplet and progress inward toward its center. This predicted inward propagation of the delamination front is in remarkable contrast to the outward propagation that is observed when ablation of a

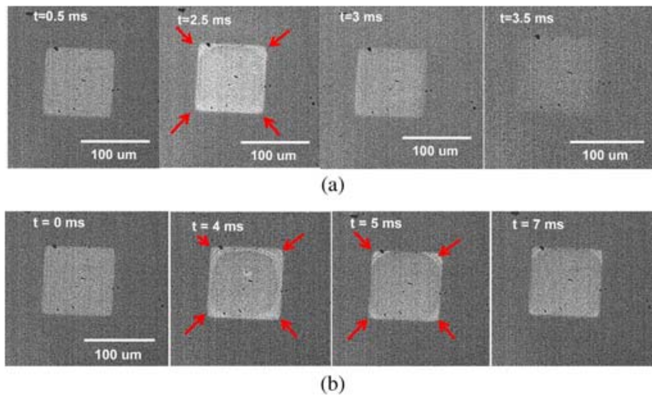

Fig. 6. Frames from a high-speed film showing (a) the delamination process that starts at the corners (frame 2) and progresses toward the center resulting in the 100-μm Si chiplet leaving the transfer tool and (b) a partial delamination event in which the delamination front begins moving toward the center from the corners before reversing directions. The chiplet remains adhered to the transfer tool. (a) Complete delamination. (b) Incomplete delamination.

sacrificial layer or the transfer tool material is the mechanism driving the delamination and ejection of the microstructure (see [18]).

To observe the previously suggested delamination mechanism, the placement machine's high-resolution camera was replaced with a high-speed camera (Phantom v7.3). Preliminary tests indicated that the illumination produced by the laser pulse was sufficient to produce adequate contrast in the image frames of the camera at speeds up to around 2500 fps. Fig. 6(a) shows four frames recorded when working with the laser set to produce a flux of 10 W for an interval of 0.004 s at the transfer-tool–chiplet interface. In the frame taken at 2.5 ms after the start of the laser pulse, the delamination process can be clearly observed to have started at the corners of the chiplet and progressed some distance inward. By 3 ms, the chiplet has released from the transfer tool and moved out of focus of the camera (i.e., transferred onto the substrate by 3.5 ms). To better observe the progress of the delamination front, the laser power was gradually decreased to a point where there is not enough strain energy release to drive the delamination to completion. Fig. 6(b) shows a situation, observed at a laser power flux of 8 W for 0.004 s, where the delamination front is seen to develop at the corners and propagate inward toward the center of the chiplet but then retract back to the edges and corners, suggesting insufficient strain energy release to complete the delamination of the chiplet from the transfer tool. The transfer tools used in the process were observed under a microscope before and after placement. For the placement conditions described in the aforementioned experiments, no damage could be visually observed. Also, the same transfer tool was used for multiple placement experiments, and no change in placement (pickup or depositing) was observed.

The observations of the initiation of the delamination front at the outside edges of the chiplet and its propagation toward the center, along with the fact that the transfer tool is not damaged and can be used repeatedly for pickup and placement operations, suggest a thermomechanical phenomenon rather than the ablation of the polymeric transfer tool material at the interface.

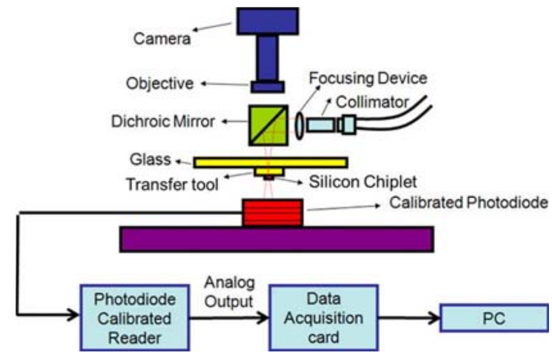

Fig. 7. Laser energy incident on the chiplet is measured by the difference in energy arriving at a calibrated photodiode with and without the chiplet present on the transfer tool.

IV. Thermomechanical Fracture Mechanics Model for LMTP

To verify the plausibility of the mechanism proposed, we measure the amount of radiation absorbed by the chiplet during a typical laser pulse that is used for placement. We then use this as the input for a numerical model to determine the temperature of the chiplet and the transfer tool at, and around, the tool–chiplet interface. This is used in an analytical model to compute if it leads to an energy release rate at the transfer-tool–chiplet interface that exceeds the work of adhesion between the materials of chiplet and the transfer tools. Finally, a scaling law for delamination of the chiplet from the transfer tool is established, which governs the critical time for delamination.

To measure the heat flux available in a laser pulse used for delamination, the receiving substrate is replaced with a photodiode power meter (Thorlabs S142C), as shown in Fig. 7. The rest of the setup is maintained exactly the same, as originally shown in Fig. 3. The laser beam travels through the optical fiber, collimator, and focusing lens, and the dichroic mirror reflects the focused laser beam to the chiplet (100 μm × 100 μm × 3 μm silicon chip). Part of the laser beam energy that is incident on the chiplet is absorbed by it, and the rest is reflected away by its surface. The remaining energy in the beam passes around the chiplet (with some fraction transmitted through the 3-μm thickness of the chiplet) and is captured by the photodiode power meter. This power meter is chosen to have a very fast response time (< 200 ns) compared to the laser pulsewidth (4 ms), high optical power range (5 μW–5 W) to withstand the intensity of the beam, high resolution (1 nW), and large aperture (∅12 mm) to be able to easily capture the entire laser beam. The photodiode power signal is then translated to laser power utilizing a precalibrated reader (Thorlabs PM100D). A data acquisition card captures the analog output of the calibrated reader at a sampling rate of 40 kHz and stores it on a PC for subsequent analysis.

This experiment is performed in two steps. In the first stage, the chiplet is loaded on the transfer tool and subjected to a 4-ms laser pulse with intensity just below that needed to produce delamination. The photodiode power meter measures the energy in the laser pulse that passes around and through the chiplet. In the second step of this measurement, the chiplet is removed from the transfer tool, and the same 4-ms laser

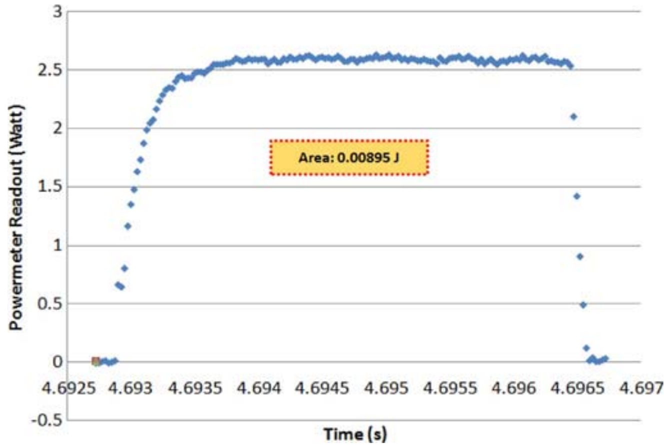

Fig. 8. Power measurements with the chiplet on the transfer tool for a single 4-ms-long laser pulse.

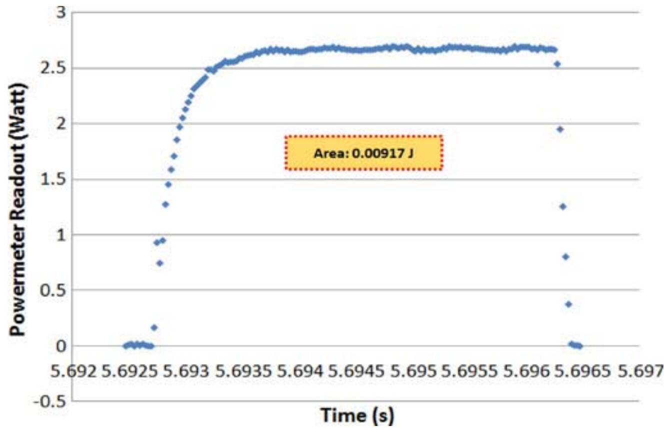

Fig. 9. Power measurement with no chiplet on the transfer tool for a single 4-ms-long laser pulse.

pulse is sent to the transfer tool with the photodiode power meter measuring the energy in the laser pulse that emerges out from the transfer tool. The difference between these two measurements is the energy in the pulse that is absorbed or reflected away by the chiplet.

Figs. 8 and 9 show the power meter measurements with and without the chiplet on the transfer tool, respectively. As shown in Fig. 8, the photodiode power meter receives 0.00895 J during a 4-ms laser pulse with the chiplet loaded on the transfer tool, and as shown in Fig. 9, it receives 0.00917 J for the identical laser pulse when there is no chiplet loaded on the transfer tool. Therefore, the incident energy to the silicon chiplet during a 4-ms laser pulse is 0.224 mJ, the difference between these two values. With a reflectivity of 0.328 for polished silicon [19], the energy absorbed by the silicon chiplet is 0.151 mJ. This energy heats up the chiplet and the PDMS of the transfer tool across the contact interface to drive the delamination.

A finite element model [20] is used in the transient heat transfer analysis to determine the temperature field. The top surface of the glass backing layer of the transfer tool is fixed, and the top surface of the silicon chiplet is constrained to move with the bottom surface of the post on the PDMS transfer tool. Other surfaces in this model are free to move, with the air

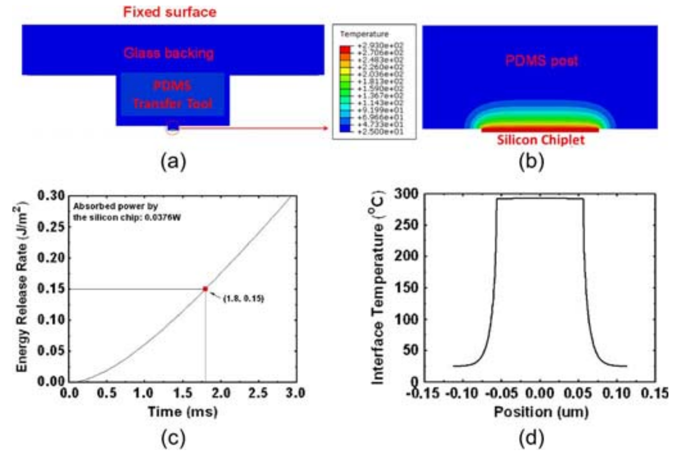

Fig. 10. (a) Finite element model of the transfer placement system. (b) Temperature distribution in the post and attached chiplet at 1.8 ms. (c) Energy release rate distribution with time. (d) Temperature distribution along the transfer-tool–chiplet interface.

cooling boundary conditions and the coefficient of natural convection of $25\ \mathrm{W}\cdot\mathrm{m}^{-2}\cdot\mathrm{K}^{-1}$ [21]. Other material parameters, including specific heat, heat conductivity, coefficient of thermal expansion, mass density, elastic modulus, and Poisson's ratio, are given explicitly in Section IV. As has been explained earlier, the silicon chiplet absorbs part of the incident laser energy and behaves as a heat source and, as indicated by our experimental measurements, inputs 0.151 mJ of energy over a 4-ms interval, i.e., 0.0376 W of power, at the transfer-tool–chiplet interface. Finite element analysis (FEA) is performed for a 4-ms interval of time. An axisymmetric model is used, and hence, the equivalent radius of the silicon chiplet is 56 μm with the same in-plane area as the 100 μm $\times$ 100 μm square chiplet.

Fig. 10(a) and (b) shows the temperature distribution in the cross section cut along the center line of the chiplet at 1.8 ms. It reaches the maximum in the silicon and decreases rapidly in the PDMS because of the high and low coefficients of thermal conductivity for silicon and PDMS, respectively. At the time of 1.8 ms, the delamination starts because the finite element model for the thermomechanical fracture analysis gives the energy release rate [Fig. 10(c)] reaching the work of adhesion of 0.15 J/m^2 for silicon–PDMS interface reported in the literature [22]. The FEA also shows that the silicon chiplet undergoes much smaller deformation than the PDMS. This is because the coefficient of thermal expansion for silicon (2.6×10^{-6} K^{-1}[17]) is two orders of magnitude smaller than that of PDMS (3.1×10^{-4} K^{-1}[16]). This thermal mismatch provides the driving force for the delamination process. Fig. 10(d) shows an almost uniform temperature in the chiplet but a sharp drop to room temperature immediately outside the chiplet (because of the low thermal conductivity of PDMS).

An analytical model is developed to establish a scaling law governing the delamination of silicon chiplet from the PDMS post. For simplicity, an axisymmetric model is adopted for the system of the PDMS post and silicon chip (Fig. 11), where $r_{\mathrm{silicon}} = 56\ \mu$m is the equivalent radius for the square silicon chiplet by enforcing the same in-plane area and $h_{\mathrm{silicon}} = 3\ \mu$m is the thickness of the silicon chip. The heat source is modeled as a disk with a radius r_{silicon} and total heat generation

the same as that absorbed by the silicon chip. The PDMS is modeled as a semi-infinite solid. Hankel transform and Fourier cosine transform are applied in the radial and axial directions, respectively, to solve the transient heat conduction equation. The temperature distribution is obtained from the transient heat conduction equation $(\partial^2 \Delta T_{\mathrm{PDMS}}/\partial r^2) + (1/r)(\partial \Delta T_{\mathrm{PDMS}}/\partial r) + (\partial^2 \Delta T_{\mathrm{PDMS}}/\partial z^2) = (c_{\mathrm{PDMS}}\rho_{\mathrm{PDMS}}/\lambda_{\mathrm{PDMS}})(\partial \Delta T_{\mathrm{PDMS}}/\partial t)$ in cylindrical coordinates (r, z) with the initial condition $\Delta T_{\mathrm{PDMS}}|_{t=0} = 0$, where ΔT_{PDMS} is the temperature rise in PDMS from the ambient temperature and $c_{\mathrm{PDMS}} = 1460\ \mathrm{J \cdot kg^{-1} \cdot K^{-1}}$, $\rho_{\mathrm{PDMS}} = 970\ \mathrm{kg \cdot m^{-3}}$, and $\lambda_{\mathrm{PDMS}} = 0.15\ \mathrm{W \cdot m^{-1} \cdot K^{-1}}$ are the specific heat, mass density, and heat conductivity of PDMS, respectively [16]. The full temperature distribution ΔT_{PDMS} then induces a nonuniform field of thermal strain $\alpha_{\mathrm{PDMS}}\Delta T_{\mathrm{PDMS}}$ in PDMS via its coefficient of thermal expansion α_{PDMS}. The thermal strain in the silicon chiplet is negligibly small since its coefficient of thermal expansion is two orders of magnitude smaller than that of PDMS. For an interface crack between the PDMS and silicon chiplet, its energy release rate G subject to the nonuniform field of thermal strain (misfit strain) $\alpha_{\mathrm{PDMS}}\Delta T_{\mathrm{PDMS}}$ is then obtained analytically by the integration of its Green's function for a point dilatation [23]. Once the energy release rate G reaches the work of adhesion γ of the transfer-tool–chiplet interface, i.e., $G = \gamma$, the interface delaminates, which gives the absorbed laser power P of the silicon chip as a function of critical time t for delamination

$$\frac{P\alpha_{\mathrm{PDMS}}}{\lambda_{\mathrm{PDMS}}}\sqrt{\frac{\mu_{\mathrm{PDMS}}}{r_{\mathrm{silicon}}\gamma}} = f\left(\frac{\lambda_{\mathrm{PDMS}}t}{c_{\mathrm{PDMS}}\rho_{\mathrm{PDMS}}r_{\mathrm{silicon}}^2}, \frac{c_{\mathrm{silicon}}\rho_{\mathrm{silicon}}h_{\mathrm{silicon}}}{c_{\mathrm{PDMS}}\rho_{\mathrm{PDMS}}r_{\mathrm{silicon}}}\right) \quad (1)$$

where $\alpha_{\mathrm{PDMS}} = 3.1 \times 10^{-4}\ \mathrm{K^{-1}}$, $\mu_{\mathrm{PDMS}} = 0.67$ MPa is the shear modulus of PDMS, and $c_{\mathrm{silicon}} = 708\ \mathrm{J \cdot kg^{-1} \cdot K^{-1}}$ and $\rho_{\mathrm{silicon}} = 2300\ \mathrm{kg \cdot m^{-3}}$ are the specific heat and mass density of the silicon chip, respectively [16], [24]. This suggests that the normalized absorbed laser power $(P\alpha_{\mathrm{PDMS}}/\lambda_{\mathrm{PDMS}})\sqrt{\mu_{\mathrm{PDMS}}/(r_{\mathrm{silicon}}\gamma)}$ depends on the normalized critical time for delamination $\lambda_{\mathrm{PDMS}}t/(c_{\mathrm{PDMS}}\rho_{\mathrm{PDMS}}r_{\mathrm{silicon}}^2)$ via a single nondimensional combination of the specific heat and mass density of silicon and PDMS and the aspect ratio of the silicon chiplet $c_{\mathrm{silicon}}\rho_{\mathrm{silicon}}h_{\mathrm{silicon}}/(c_{\mathrm{PDMS}}\rho_{\mathrm{PDMS}}r_{\mathrm{silicon}})$. The function f in (1) is obtained analytically and involves a number of integrals that have to be evaluated numerically to produce the curve shown in Fig. 12 with $c_{\mathrm{silicon}}\rho_{\mathrm{silicon}}h_{\mathrm{silicon}}/(c_{\mathrm{PDMS}}\rho_{\mathrm{PDMS}}r_{\mathrm{silicon}}) = 0.0616$ for the situation being modeled. The analytical approach for establishing (1) and the function f will be published elsewhere. For the situation reported in the experiment, $P = 0.0376$ W was used in the FEA, which gave the critical time for delamination to be 1.8 ms. This is indicated by the circular red dot on the graph, agreeing well with the analytical model's prediction.

To further verify the scaling law, an experiment was conducted in which the pulse time was kept constant and the laser power was gradually increased until delamination occurred. The incident power of the silicon chip corresponding to these

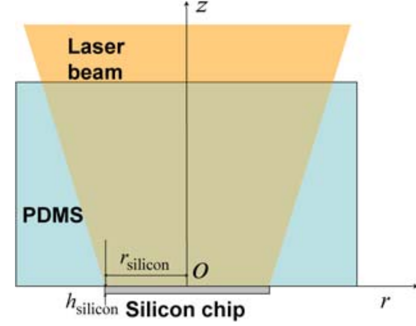

Fig. 11. Analytic model for delamination of transfer-tool–chiplet interface.

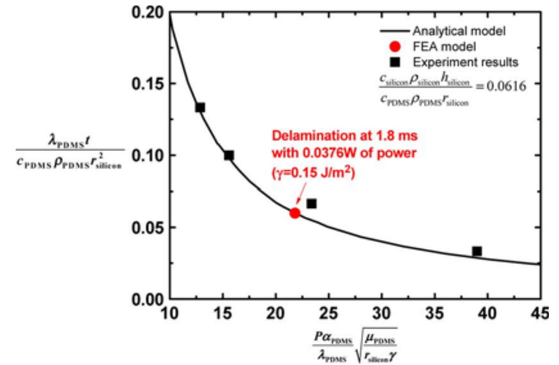

Fig. 12. Scaling law for delamination of transfer-tool–chiplet interface.

conditions was measured as previously described at the beginning of this section (see Fig. 7). In this manner, the incident power necessary for complete delamination was obtained for pulsewidths ranging from 1 to 4 ms. Taking the pulsewidth as a rough approximation of the start of delamination (in fact, this would be a slight overestimation of delamination time, because when complete delamination occurred, it typically occurred within a 0.5-ms interval), the black squares are plotted on the graph in Fig. 12. For pulsewidths of 1, 2, 3, and 4 ms, the corresponding absorbed laser powers by the silicon chip in the experiments were 0.0672, 0.0403, 0.0269, and 0.0222 W, respectively. These suggest that the experimentally observed delamination times agree well with the scaling law obtained from the analytical model.

V. Conclusion and Discussion

We have focused a millisecond laser pulse from a near-IR diode laser with power in the tens of watts at the interface between a transparent transfer tool (of PDMS) and absorbing microstructures (of SCS, GaAs, and GaN) or chiplets that have a difference of about two orders of magnitude in the coefficient of thermal expansion. The strain energy release rate generated at the transfer-tool–chiplet interface is sufficient to overcome the work of adhesion at the interface and, therefore, results in the release and transfer of the microstructure from the transfer tool to a nearby receiving substrate. We have provided high-speed photography evidence that clearly shows the delamination process as resulting from the elastic mismatch strain when the temperature of the transfer-tool/chiplet system is raised.

Measurements of IR flux incident on the chiplet, coupled with analytical and numerical models, further validate our approach.

Because the transfer tool is not damaged during this process, it is possible to use this as the basis of a simple pick-and-place assembly process for assembling 3-D microstructures that cannot easily be fabricated by other processes, as well as for printing functional microstructures into different substrates to enable emerging technologies such as flexible and stretchable electronics. This ability to transfer microstructures from a PDMS transfer tool to different receiving substrates has been integrated into a placement machine by creating a laser placement head and installing it into a computer-controlled positioning stage. The full placement cycle, i.e. extracting microstructures from the growth/fabrication substrate and assembling them on a receiving substrate, has been successfully implemented and demonstrated for a number of cases where such transfer placement would be difficult, if not impossible.

One challenge in laser-driven transfer placement is to reduce the temperatures at which delamination and transfer occur. Increasing the laser power increases strain energy release rate and facilitates delamination at the transfer-tool-chiplet interface. However, it also increases the temperatures of the chiplet and the transfer tool. The analytical and numerical models in Section IV suggest that the effective methods to reduce the transfer tool temperature include increasing the elastic modulus, coefficients of thermal expansion and thermal conductivity, specific heat, mass density, and thickness of the chiplet. Decreasing the specific heat and mass density of the transfer tool material also helps to reduce the temperatures reached during the process.

Work remains to be done in further modeling the process to be able to more accurately characterize its dynamics. Predictive models that help select appropriate process parameters for given chiplet materials and geometries are necessary. A proper characterization of the process domain along with tool development to address issues such as accuracy, rates, and yield is necessary. Also, important process parameters need to be identified, and their effect on the process needs to be quantified. For example, the precision in placement is dependent on a number of setup factors such as precise centering of the beam on the chiplet. It is also dependent on process variables, the standoff distance of the transfer tool from the receiving substrate being one of them. In initial experiments, to characterize this dependence, placement was performed at the lowest energy for reliable delamination (4-ms pulses with the current setting adjusted to produce 2.5 W at the transfer tool and the same 100 μm $\times$ 100 μm $\times$ 3 μm Si chiplets) with different standoff heights onto a substrate patterned with fiducials. First, the transfer tool, loaded with a chiplet, is brought close to the substrate and aligned to the fiducials on the substrate using the optics on the placement machine (about 1-μm resolution) and the positioning stages (also 1-μm resolution). It is then withdrawn to the appropriate height, and the chiplet is transferred to the substrate. The error in the placement process is obtained through image analysis of frames taken after alignment (with the chiplet still on the transfer tool) and after placement. This experiment is conducted for different standoff heights ranging from 5 to 300 μm, with five repetitions at each standoff height. Fig. 13 shows the observed dependence of placement errors on standoff height. Within the resolution of experimental observations, the transfer errors become insignificant at standoff heights of about 20 μm. Extensive parametric studies of this nature are yet to be conducted. Nevertheless, it is our opinion that this process has the potential to open up new pathways to assembly and packaging of MEMS and other active micro- and nanosystems.

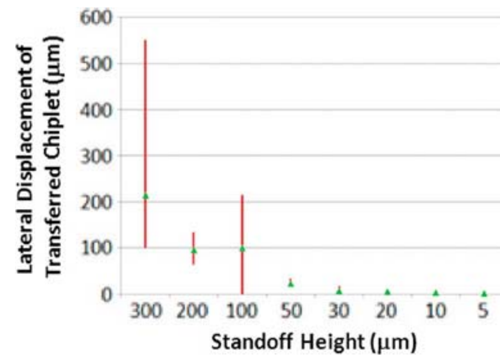

Fig. 13. Maximum lateral error observed as a function of standoff distance of the transfer tool from the receiving substrate.

Acknowledgment

The materials presented here are based upon work supported by the Center for Nanoscale Chemical–Electrical–Mechanical Manufacturing Systems, a nanoscale science and engineering center sponsored by the National Science Foundation under Award 0749028 [Civil, Mechanical, and Manufacturing Innovation (CMMI)]. The work involving nanomembranes and systematic studies of the physics relied on support by Multidisciplinary University Research Initiative from the Air Force Office of Scientific Research. The authors would also like to thank Dr. J. Soares and Dr. P. Lynch for their assistance with the laser setup, N. Ahmed, S. Elgan, and A. Carlson for their help with the placement machine, and Dr. S. Kim for his help with fabricating the chiplets and polydimethylsiloxane placement tools.

References

[1] D.-H. Kim, N. Lu, R. Ma, Y.-S. Kim, R.-H. Kim, S. Wang, J. Wu, S. M. Won, H. Tao, A. Islam, K. J. Yu, T.-I. Kim, R. Chowdhury, M. Ying, L. Xu, M. Li, H.-J. Chung, H. Keum, M. McCormick, P. Liu, Y.-W. Zhang, F. G. Omenetto, Y. Huang, T. Coleman, and J. A. Rogers, "Epidermal electronics," *Science*, vol. 333, no. 6044, pp. 838–843, Aug. 2011.

[2] S.-I. Park, Y. Xiong, R.-H. Kim, P. Elvikis, M. Meitl, D.-H. Kim, J. Wu, J. Yoon, C.-J. Yu, Z. Liu, Y. Huang, K.-C. Hwang, P. Ferreira, X. Li, K. Choquette, and J. A. Rogers, "Printed assemblies of inorganic light-emitting diodes for deformable and semitransparent displays," *Science*, vol. 325, no. 5943, pp. 977–981, Aug. 2009.

[3] H. C. Ko, M. P. Stoykovich, J. Song, V. Malyarchuk, W. M. Choi, C.-J. Yu, J. B. Geddes, J. Xiao, S. Wang, Y. Huang, and J. A. Rogers, "A hemispherical electronic eye camera based on compressible silicon optoelectronics," *Nature*, vol. 454, no. 7205, pp. 748–753, Aug. 2008.

[4] R.-H. Kim, D.-H. Kim, J. Xiao, B. H. Kim, S.-I. Park, B. Panilaitis, R. Ghaffari, J. Yao, M. Li, Z. Liu, V. Malyarchuk, D. G. Kim, A.-P. Le, R. G. Nuzzo, D. L. Kaplan, F. G. Omenetto, Y. Huang, Z. Kang, and J. A. Rogers, "Waterproof AlInGaP optoelectronics on stretchable substrates with applications in biomedicine and robotics," *Nat. Mater.*, vol. 9, no. 11, pp. 929–937, Nov. 2010.

[5] C. A. Bower, E. Menard, and E. Bonafede, "Active-matrix OLED display backplanes using transfer-printed microscale integrated circuits," in *Proc. 60th Electron. Compon. Technol. Conf.*, San Diego, CA, 2010, pp. 1339–1343.

[6] R. Wartena, A. E. Curtright, C. B. Arnold, A. Piqué, and K. E. Swider-Lyons, “Li-ion microbatteries generated by a laser direct-write method,” *J. Power Sources*, vol. 126, no. 1/2, pp. 193–202, 2004.
[7] J. Bohandy, B. F. Kim, and F. J. Adrian, “Metal deposition from a supported metal film using an excimer laser,” *J. Appl. Phys.*, vol. 60, no. 4, p. 1538, Aug. 1986.
[8] A. S. Holmes and S. M. Saidam, “Sacrificial layer process with laser-driven release for batch assembly operations,” *J. Microelectromech. Syst.*, vol. 7, no. 4, pp. 416–422, Dec. 1998.
[9] Y.-L. Loo, D. V. Lang, J. A. Rogers, and J. W. P. Hsu, “Electrical contacts to molecular layers by nanotransfer printing,” *Nano Lett.*, vol. 3, no. 7, pp. 913–917, Jul. 2003.
[10] J. Zaumseil, M. A. Meitl, J. W. P. Hsu, B. Acharya, K. W. Baldwin, Y.-L. Loo, and J. A. Rogers, “Three-dimensional and multilayer nanostructures formed by nanotransfer printing,” *Nano Lett.*, vol. 3, no. 9, pp. 1223–1227, Sep. 2003.
[11] E. Menard, L. Bilhaut, J. Zaumseil, and J. A. Rogers, “Improved chemistries, thin film deposition techniques and stamp designs for nanotransfer printing,” *Langmuir*, vol. 20, no. 16, pp. 6871–6878, Aug. 2004.
[12] M. A. Meitl, Y. Zhou, A. Gaur, S. Jeon, M. L. Usrey, M. S. Strano, and J. A. Rogers, “Solution casting and transfer printing single-walled carbon nanotube films,” *Nano Lett.*, vol. 4, no. 9, pp. 1643–1647, Sep. 2004.
[13] Y. Sun and J. A. Rogers, “Fabricating semiconductor nano/microwires and transfer printing ordered arrays of them onto plastic substrates,” *Nano Lett.*, vol. 4, no. 10, pp. 1953–1959, Oct. 2004.
[14] A. Pique, S. Mathews, R. Auyeung, and B. P. Sood, “Laser-based technique for the transfer and embedding of electronic components and devices,” U.S. Patent 8 056 222, Nov. 15, 2011.
[15] M. S. Meitl, Z. T. Zhu, V. Kumar, K. J. Lee, X. Feng, Y. Y. Huang, I. Adesida, R. G. Nuzzo, and J. A. Rogers, “Transfer printing by kinetic control of adhesion to an elastomer stamp,” *Nat. Mater.*, vol. 5, no. 1, pp. 33–38, Jan. 2006.
[16] J. E. Mark, Ed., *Polymer Data Handbook*. New York: Oxford Univ. Press, 1999.
[17] Y. Okada and Y. Tokumaru, “Precise determination of lattice parameter and thermal expansion coefficient of silicon between 300 and 1500 K,” *J. Appl. Phys.*, vol. 56, no. 2, pp. 314–320, Jul. 1984.
[18] S. G. Koulikov and D. D. Dlott, “Ultrafast microscopy of laser ablation of refractory materials: Ultralow threshold stress-induced ablation,” *J. Photochem. Photobiol. A, Chem.*, vol. 145, no. 3, pp. 183–194, Dec. 2001.
[19] M. A. Green and M. J. Keevers, “Optical properties of intrinsic silicon at 300 K,” *Progr. Photovoltaics*, vol. 3, no. 3, pp. 189–192, 1995.
[20] Dassault Systèmes, *ABAQUS Analysis User’s Manual V6.9*, Pawtucket, RI, 2009.
[21] F. P. Incropera, D. P. DeWitt, T. L. Bergman, and A. S. Lavine, *Fundamentals of Heat and Mass Transfer*. Hoboken, NJ: Wiley, 2007.
[22] S. Kim, J. Wu, A. Carlson, S. H. Jin, A. Kovalsky, P. Glass, Z. Liu, N. Ahmed, S. L. Elgan, W. Chen, P. M. Ferreira, M. Sitti, Y. Huang, and J. A. Rogers, “Microstructured elastomeric surfaces with reversible adhesion and examples of their use in deterministic assembly by transfer printing,” *Proc. Nat. Acad. Sci. USA*, vol. 107, no. 40, pp. 17 095–17 100, Oct. 2010.
[23] Z. Suo, “Singularities interacting with interfaces and cracks,” *Int. J. Solids Struct.*, vol. 25, no. 10, pp. 1133–1142, 1989.
[24] S. A. Campbell, *The Science and Engineering of Microelectronic Fabrication*. New York: Oxford Univ. Press, 2001.

Reza Saeidpourazar received the B.S. degree in mechanical engineering from Khajeh Nasir Toosi University of Technology, Tehran, Iran, in 2003, the M.S. degree in mechanical engineering from Sharif University of Technology, Tehran, in 2005, and the Ph.D. degree from the Department of Mechanical Engineering, Clemson University, Clemson, SC, in 2009.

From 2009 to 2011, he was a Postdoctoral Research Associate with the Center for Nanoscale Chemical–Electrical-Mechanical Manufacturing Systems, University of Illinois at Urbana-Champaign, Urbana. He is currently with Brooks Automation Inc., Chelmsford, MA. His research interests include robotics, control, automation, and micro- and nanomanufacturing.

Dr. Saeidpourazar was a recipient of the SPIE Scholarship in Optical Science and Engineering, the International Society of Automation Scholarship Award, and Clemson University’s Board of Visitors Graduate Researcher Award, Outstanding Graduate Researcher Award, and Distinguished Achievement Fellowship.

Rui Li is currently working toward the Ph.D. degree in civil engineering in the Faculty of Infrastructure Engineering, Dalian University of Technology, Dalian, China.

He is also currently a Visiting Scholar with the Department of Civil and Environmental Engineering and the Department of Mechanical Engineering, Northwestern University, Evanston, IL. His research interests include mechanics of flexible electronics, plate and shell structures, and symplectic approach for applied mechanics. He has published 20 journal papers.

Yuhang Li was born in 1983. He received the B.Sc. and M.Sc. degrees from Harbin Institute of Technology, Harbin, China, in 2006 and 2008, respectively, where he is currently working toward the Ph.D. degree in the School of Astronautics.

From 2010 to 2012, he is a visiting student with the Department of Civil and Environmental Engineering and the Department of Mechanical Engineering, Northwestern University, Evanston, IL. His research interests include structural vibration control and mechanical and heat transfer analysis of flexible electronics.

Michael D. Sangid received the B.S. degree in mechanical engineering with a minor in mathematics and the M.S. and Ph.D. degrees in mechanical engineering from the University of Illinois at Urbana-Champaign, Urbana, in 2002, 2005, and 2010, respectively.

During his undergraduate studies, he was with the Advanced Materials Testing and Evaluation Laboratory and the Autonomic Materials Laboratory, University of Illinois, where he worked in the fields of material behavior and testing. After his M.S. degree, for two years, he was with Rolls-Royce Corporation, Indianapolis, IN, specializing in material characterization, deformation, fatigue, fracture, and creep of high-temperature aerospace materials, before resuming his education in 2007. His research has centered around a multiscale approach to understand grain boundary effects on crack initiation. Through this work, atomistic simulations are used to quantify local energy barriers to deformation, which are built into continuum models to connect material structure to performance. He was a Postdoctoral Research Associate with the University of Illinois, where he worked on the following: 1) heterogeneous deformation of materials and fatigue crack growth testing and modeling of new and emerging materials and 2) prediction of fiber orientation and length in polymer-based long fiber composites. Since the fall of 2011, he has been an Assistant Professor with the School of Aeronautics and Astronautics, Purdue University, West Lafayette, IN, where he continues his work on building computational material models with experimental verification and validation efforts.

Dr. Sangid is an active member of the Minerals, Metals, and Materials Society; American Society of Mechanical Engineers; American Institute of Aeronautics and Astronautics; ASM International; and Pi Tau Sigma Honor Society of Mechanical Engineers.

Chaofeng Lü received the B.S. degree in civil engineering and the Ph.D. degree in structural engineering from Zhejiang University, Hangzhou, China, in 2001 and 2006, respectively.

From 2007 to 2009, he was a Postdoctoral Research Fellow with the City University of Hong Kong, Kowloon, Hong Kong. He joined the faculty of the Department of Civil Engineering, Zhejiang University, in 2006, where he has been an Associate Professor since 2008 and is also currently a Key Member of the Soft Matter Research Center. From December 2009 to March 2012, he was a Visiting Scholar in the Department of Civil and Environmental Engineering and the Department of Mechanical Engineering, Northwestern University, Evanston, IL. He has published more than 40 peer-reviewed international journal papers which received over 300 self-excluded independent citations. His research interests include thermal issues in the manufacture of micro- and nanodevices, mechanics of nanostructures, and smart/composite materials and structures.

Yonggang Huang received the Ph.D. degree from Harvard University, Cambridge, MA, in 1990.

He was the Grayce Wicall Gauthier Professor (2003–2004) and the Shao Lee Soo Professor (2004–2007) at the University of Illinois at Urbana-Champaign, Urbana, the Visiting Clark Millikan Professor (2005–2006) at the California Institute of Technology, Pasadena, and an Honorary Professor at Nanjing University of Posts and Telecommunications, Nanjing, China. He is currently the Joseph Cumming Professor in the Department of Mechanical Engineering and the Department of Civil and Environmental Engineering, Northwestern University, Evanston, IL. He is interested in establishing mechanics models for advanced technology, such as stretchable electronics, flexible silicon solar cell, cardiac and neutral electrophysiology, and epidermal electronics. He has published one book, 27 book chapters, and more than 360 papers in journals, including multidisciplinary journals *Science* (2006, 2008, 2009, 2010, and 2011) and its sister journal *Science Translational Medicine* (2010), *Nature* (2008) and its sister journals *Nature Materials* (2006, 2008, 2010a, b, and 2011), *Nature Nanotechnology* (2006), *Nature Neuroscience* (2011), and *Nature Communications* (2012), and *Proceedings of the National Academy of Sciences* (2007, 2008, 2009, 2010, and 2011a, b); physics journal *Physical Review Letters* (2004 and 2010); materials journal *Advanced Materials* (2009, 2010a, b, and 2011); nanojournal *Nano Letters* (2007, 2008, 2009a, b, 2010, and 2011); and mechanics journal *Journal of the Mechanics and Physics of Solids* (38 papers). He is the Editor-in-Chief of *Theoretical and Applied Mechanics Letters* and an Editor of *Journal of Applied Mechanics* (*Transactions of the American Society of Mechanical Engineers*).

Dr. Huang has been a recipient of various awards, including the Larson Award (2003), Melville Medal (2004), and Richards Award (2010) from the American Society of Mechanical Engineers; the Young Investigator Medal (2006) from the Society of Engineering Science; the International Journal of Plasticity Medal (2007); the Guggenheim Fellowship (2008); the Institute for Scientific Information Highly Cited Researcher in Engineering (2009); and the Green Photonics Award (2011) from SPIE.

John A. Rogers (F'10) received the B.A. degree in chemistry and the B.S. degree in physics from the University of Texas at Austin, in 1989, and the S.M. degrees in physics and chemistry and the Ph.D. degree in physical chemistry from the Massachusetts Institute of Technology (MIT), Cambridge, in 1992 and 1995, respectively.

In 1997, he joined Bell Laboratories as a Member of Technical Staff, where he was the Director from the end of 2000 to 2002. He is currently the Lee J. Flory-Founder Chair in Engineering at the University of Illinois at Urbana-Champaign, Urbana, with a primary appointment in the Department of Materials Science and Engineering.

Dr. Rogers is a member of the National Academy of Engineering and a Fellow of the American Physical Society, the Materials Research Society, and the American Association for the Advancement of Science. His research has been recognized with many awards, including a MacArthur Fellowship in 2009 and the Lemelson–MIT Prize in 2011. From 1995 to 1997, he was a Junior Fellow in the Harvard University Society of Fellows.

Placid M. Ferreira received the B.E. (M.E.) degree from the University of Bombay, Mumbai, India, in 1980, the M.Tech. (M.E.) degree from the Indian Institute of Technology Bombay, Mumbai, in 1982, and the Ph.D. degree in industrial engineering from Purdue University, West Lafayette, IN, in 1987.

Since 1987, he has been a member of the mechanical engineering faculty at the University of Illinois at Urbana-Champaign, Urbana, where he was the Associate Head for graduate programs and research from 1999 to 2002 and the Director of the Center for Nanoscale Chemical–Electrical–Mechanical Manufacturing Systems, a National Science Foundation (NSF)-sponsored nanoscale science and engineering center, from 2003 to 2009. He is currently the Head of the Department of Mechanical Science and Engineering, University of Illinois at Urbana-Champaign, where he is also the Grayce Wicall Gauthier Professor. His research interests include nanomanufacturing, precision engineering, and machine tools.

Dr. Ferreira was a recipient of the NSF Presidential Young Investigator Award in 1990, the Society of Manufacturing Engineers Outstanding Young Investigator Award in 1991, and the University of Illinois University Scholar Award in 1994. He became a Fellow of the Society of Manufacturing Engineers in 2011.